

# Biocompatible Films with Tailored Spectral Response for Prevention of DNA Damage in Skin Cells

Rebeca Núñez-Lozano, Belén Pimentel, José R. Castro-Smirnov, Mauricio E. Calvo, Hernán Míguez,\* and Guillermo de la Cueva-Méndez\*

Protection from solar radiation is commonly achieved through the use of UV organic absorbers, such as benzophenones or benzotriazoles, often combined with inorganic materials such as TiO<sub>2</sub> or ZnO<sub>2</sub>, supplied in the form of submicron size particles.<sup>[1]</sup> These compounds are usually dispersed in lotions or films,<sup>[2]</sup> the latter being typically made of polymers or inorganic glasses.<sup>[3,4]</sup> Lotions are mainly employed for skin protection, whilst solid state dispersions and coatings are typically used to improve the durability of plastics, whose mechanical stability is compromised by chain scissions, chain crosslinks and chain oxidations induced by UV absorption. Accordingly, these types of films are used in the fabrication of food packaging, to preserve containers and their edible contents from UV-induced damage, and also of glasses, to impede that UV rays reach, and harm, the eye. Solid state approaches to UV shielding might also find relevant applications in the field of skin protection, as they could be integrated in all sorts of screens or epidermal patches. However, a drawback of films like the above is that UV absorption induces the generation of free radicals, which not only reduce the mechanical stability of the polymer matrix progressively but also are toxic to cells.<sup>[5-7]</sup> Overcoming the problems associated to this inappropriate stability and biocompatibility may be possible using UV-reflecting films, which have been proposed recently as an alternative to traditional UV-absorbing-based materials.<sup>[8]</sup> There, the traditionally employed UV-absorption mechanism is substituted by radiation blockage, achieved as a result of the strong reflectance that arises from optical interference effects. This optical shielding has therefore a structural origin, rather than compositional, and has the advantage of preventing the undesired effects that highly reactive chemical species produced upon UV absorption have on the films themselves and on the tissues that they intend to protect. Besides all this, an appealing feature of UV-reflecting films

is that their optical response can be tailored to measure, so that they block very efficiently any predetermined wavelength range.

In view of all the above, here we investigated the possibility of making biocompatible, flexible, and transparent UV-reflecting films, designed to block selectively the wavelength spectrum inducing genotoxic damage in human skin cells. Central materials to our design were films made of stacked porous 1D photonic crystals (1DPC) infiltrated with a biocompatible polymer.<sup>[9]</sup> The refractive index of the different constituent films of the 1DPCs can be controlled during fabrication, enabling production of multilayered structures (i.e., Bragg stacks) where this parameter changes with a predetermined periodicity along their transversal section. This type of arrangement induces optical interference effects that can be exploited to tune the reflective properties of films, so that they block light of any given wavelength range of choice. Importantly, light absorption does not occur in this type of films, thus making them a good alternative to confer UV protection without the undesired effects described above for traditional filters. In this work we produced a flexible film whose reflectance maximum matched that of UV radiation inducing erythema and genotoxic damage in vivo<sup>[10]</sup> and analyzed its shielding effect using cultured human skin cells. Our results demonstrate that this flexible Bragg stack protected cells from UV-induced DNA damage as effectively as UV-absorbing compounds embedded in similar polymer matrices. To the best of our knowledge, this constitutes the first experimental evidence of protection of epithelial cells by a biocompatible flexible film rationally designed to shield specifically against a highly genotoxic UV range and in which no absorption occurs, hence avoiding undesired secondary effects that compromise the integrity and biocompatibility of more traditional materials.

Films used in this work were prepared by stacking together three different flexible 1DPCs, as previously reported.<sup>[8]</sup> Two of these photonic crystals were made by overlaying 24 alternate sheets of ZrO<sub>2</sub> and SiO<sub>2</sub> particles, while 20 alternate sheets of TiO<sub>2</sub> and SiO<sub>2</sub> particles were overlaid instead to make the third one, in all cases using spin casting. The resulting 1DPCs were then infiltrated with polydimethylsiloxane (PDMS), which trapped the particles above inside a biocompatible polymer that is well tolerated by human tissues and widely used in medicinal and pharmaceutical applications. Then they were lifted off their original rigid substrates to attain self-standing mirrors, and stuck to each other to yield a thin (1 mm) stable film, which we labeled ZST-3. Field emission scanning electron microscopy (FESEM) was employed to confirm the multilayered structure in cross sections of our films (Figure 1a), and their overall transparency was verified by looking at multicolored backgrounds through them (Figure 1b). This transparency was also

Dr. R. Núñez-Lozano, Dr. B. Pimentel,  
Dr. G. de la Cueva-Méndez  
Synthetic Biology and Smart Therapeutic Systems Group  
Andalusian Centre for Nanomedicine and  
Biotechnology (BIONAND)  
Parque Tecnológico de Andalucía  
C/Severo Ochoa 35, 29590 Campanillas, Málaga, Spain  
E-mail: gdelacueva@bionand.es



Dr. J. R. Castro-Smirnov, Dr. M. E. Calvo, Prof. H. Míguez  
Multifunctional Optical Materials Group  
Institute of Materials Science of Sevilla  
Spanish National Research Council-University of Sevilla  
C/Américo Vesputio 49, 41092 Sevilla, Spain  
E-mail: h.miguez@csic.es

DOI: 10.1002/adhm.201500223

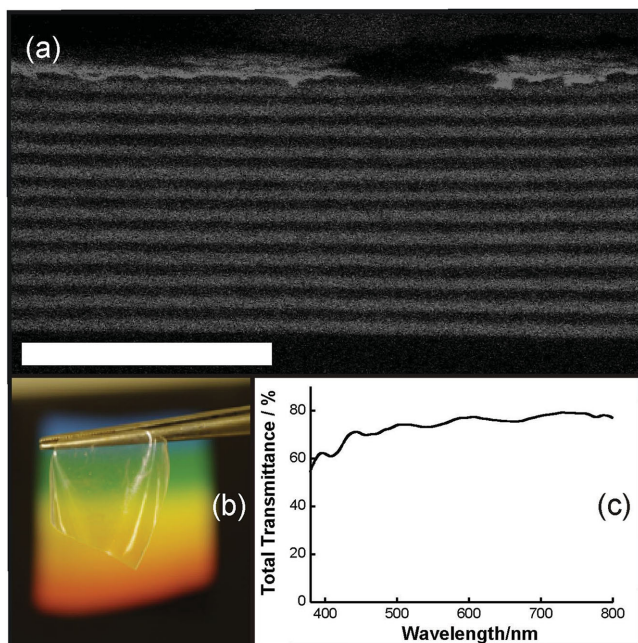


**Figure 1.** a) FESEM image of the cross section of one of the flexible periodic multilayers contained in the UV protecting stack. The scale bar is 500 nm. b) Picture of a rainbow colored background seen through the ZST-3 film. c) Total transmittance spectrum of the ZST-3 film in the visible region of the spectrum.

confirmed measuring the total transmittance of ZST-3 film, which showed spectral values ranging between 70% and 80% in the visible region of the electromagnetic spectrum (Figure 1c). We also measured the reflectance spectra of the three constituent flexible mirrors before (Figure 2a) and after (Figure 2b) adhering them together. This revealed a good match between the reflectance of the ZST-3 film and the targeted action spectrum, i.e., the wavelength range reported to induce genotoxic damage in skin cells,<sup>[10]</sup> also plotted in Figure 2b (red solid line). The composition and stacking order of the three mirrors were carefully chosen to ensure that the resulting film displayed minimum light absorption at targeted UV wavelengths and maximum transparency in the visible range. In order to achieve this, light must encounter first the  $\text{ZrO}_2\text{-SiO}_2$  mirrors and then the  $\text{TiO}_2\text{-SiO}_2$  one. To confirm the above, we analyzed the absorbance and transmittance spectra of ZST-3, which showed that barely any light was absorbed by the film in the wavelength range inducing DNA damage in skin cells, and that the transparency of the film to visible light was considerably well preserved, with transmittance values above 70% in the range 450–790 nm (see Figure 1c). The main purpose of our work was to compare the performance of the rationally designed ZST-3 UV-reflecting film with that of traditional (i.e., UV absorbing) ones. Therefore we also produced one of the latter films, embedding a 500 nm thick layer of packed  $\text{TiO}_2$  particles (i.e., equivalent to the total thickness of  $\text{TiO}_2$  nanoparticles present in the ZST-3 film) in a 1 mm thick PDMS sheet. Following this, we confirmed that, as expected, the resulting film (T-1) absorbed light in the DNA-damaging wavelength range (Figure 2d), making it an appropriate reference control in our following experiments using cultured human skin cells.

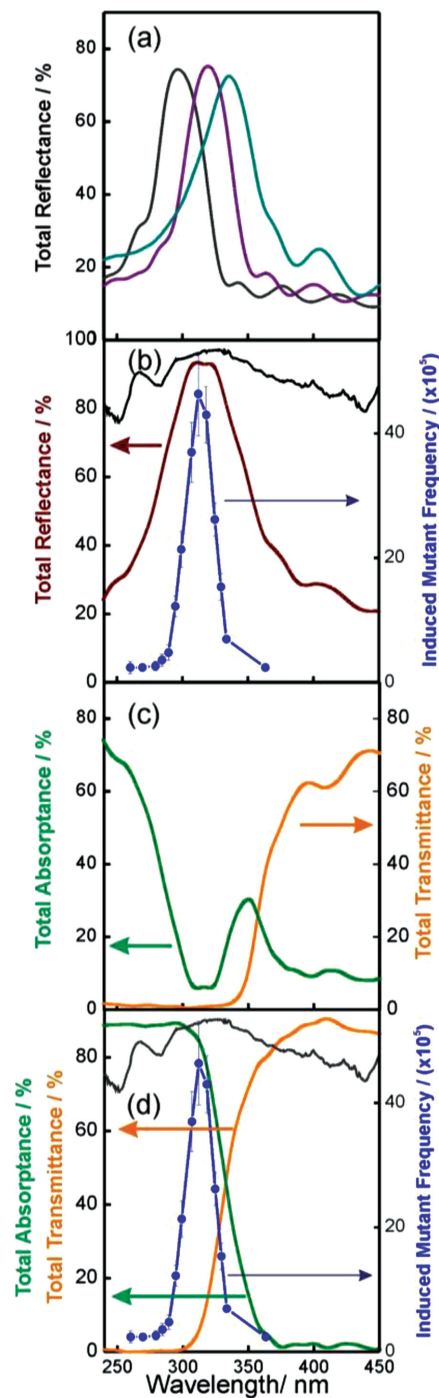


**Figure 2.** a) Reflectance spectra of the three 1DPCs used to make the ZST-3 film. Dark gray and violet curves correspond to  $\text{ZrO}_2\text{-SiO}_2$  mirrors, while the cyan curve corresponds to  $\text{TiO}_2\text{-SiO}_2$  multilayers. b) Reflectance spectrum of the ZST-3 film (dark red solid line) superimposed to the action spectra of UV-induced genotoxicity in the skin (blue solid line) reported by Ikehata and co-workers,<sup>[10]</sup> and the spectral irradiance of the lamp (black solid line). c) Absorbance (green solid line) and total (diffuse plus ballistic) transmittance (orange solid line) for the ZST-3 film. d) Total (diffuse plus ballistic) transmittance (orange solid line) and absorbance (green solid line) for the T-1 film superimposed to the action spectrum of UV genotoxicity in the skin (blue solid line) reported by Ikehata and co-workers,<sup>[10]</sup> and the spectral irradiance of the lamp (black solid line).

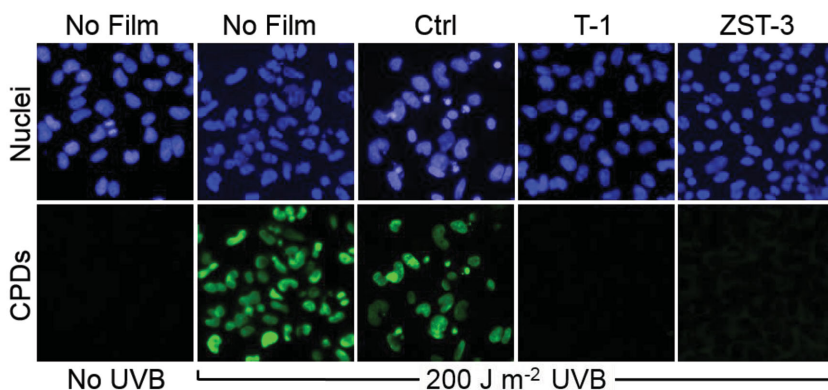


**Figure 3.** Fluorescent microscopy images showing nuclear staining (top) and CPD staining (bottom) of SB2 samples taken 15 h after being exposed to UVB radiation in the doses indicated below the bottom panels, whilst covered by the films indicated above the top panels.

First, we analyzed the extent to which the films above could protect cells against the genotoxic effects of UV radiation. Exposure of cells to UV harms their DNA and this can lead to cell death (if damage is excessive) or cellular transformation (if damage induces genomic mutations that confer neoplastic or malignant traits to cells). Cyclobutane pyrimidine dimers (CPDs) are the most frequent premutagenic DNA lesions produced by UV radiation in human cells.<sup>[11,12]</sup> CPDs can be detected using specific antibodies, which enabled us to analyze whether our filters protected cells from UV-induced genotoxicity. To do this we irradiated cultured human skin (SB2) cells with  $200 \text{ J m}^{-2}$  UV using a broad band UV lamp, and compared the frequency and intensity of CPD signals in unprotected samples with those observed in samples protected with films T-1, ZST-3, or a control (Ctrl) film made only of PDMS, as well as in nonirradiated samples. A very strong CPD-positive signal was observed in the nuclei of irradiated cells when either no film or the control film was used. In contrast, no CPD signal was detected in cells that were placed under the UV-absorbing T-1 film during irradiation. Importantly, the same result was obtained in cells that had been placed under the ZST-3 film during UV exposure (Figure 3). These observations revealed that the strong UV-reflecting behavior of the flexible multilayered ZST-3 film protects human skin cells against UV-induced DNA damage as much as the UV-absorption mechanism typical of traditional films.

To test this further, we also analyzed the rates of cell death in cultures that had been exposed to UV radiation, and whether these changed when cultures were placed under the films above during irradiation. When CPDs appear, cells arrest proliferation and activate mechanisms to repair these lesions. If they succeed, the cell cycle is restored and proliferation resumes. However, in cells where DNA damage is irreparable a programmed cell death mechanism, termed apoptosis,<sup>[13]</sup> is activated, which helps to eliminate potentially cancerous cells. A direct correlation exists between the irradiation dose, the amount of DNA damage caused, and the ability of cells to repair the latter. Consequently, the higher the ultraviolet B (UVB) dose cells receive, the more likely is that they suffer an irreparable damage and activate apoptosis. Thus, we asked whether the ZST-3 film could reduce apoptotic rates in SB2 cells exposed

to higher doses of UV radiation. To test this we irradiated SB2 cultures placed under the ZST-3 film, or the T-1 film, or none of them, with  $1000 \text{ J m}^{-2}$  UV, and let cells repair their DNA, if required, for 15 h, before counting apoptotic cells in our samples (Figure 4). This showed that the proportion UV-induced apoptosis in unprotected SB2 cells was 11.9% (median value), which was considerably higher than the background cell death rates (0.7%) observed in nonirradiated control samples. Reassuringly, covering cells with the ZST-3 film during irradiation reduced apoptosis rates to background levels again (0.7%), as it happened also in the case of the T-1 film (0.2%; Figure 4b). These results confirmed that the UV-reflecting behavior tailored into the ZST-3 film conferred a very effective protection against the noxious effects of UV radiation in cells, even when the latter was applied in high doses.

In summary, in this work we show that the ordered stacking of three multilayered 1DPCs with refractive indexes varying periodically and precisely across their transversal section produces a flexible and biocompatible film that is transparent to visible light but behaves as a highly reflective mirror for DNA-damaging UV radiation. Rather than to replace sunscreen lotions, these films are intended as dermal care products that confer both physical and radiation protection while preserving

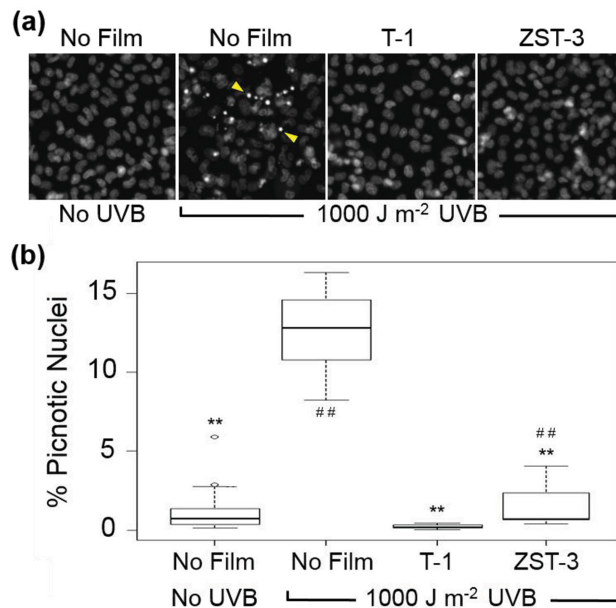


**Figure 4.** a) Fluorescent microscopy images showing nuclear staining of SB2 samples taken 15 h after being exposed to UVB radiation in the doses indicated below the bottom panels, whilst covered by the films indicated above the top panels. A couple of the picnotic nuclei observed in irradiated unprotected cells are highlighted using yellow arrowheads. b) Box-and-whisker plot showing the percentage of picnotic nuclei found in the samples above. Values show statistical significance (\*\* $p < 0.01$ , when compared to no film- $1000 \text{ J m}^{-2}$  and ## $p < 0.01$  when compared to T-1 film).

the visibility of the areas where they could be applied, such ill, burnt, or wounded skin. Accordingly, we demonstrate that this film protects cultured human skin cells from UV-induced DNA lesions and from the lethal consequences that overwhelming doses of UV radiation have for cells. The mechanism of protection in this film is based on UV reflection, induced by optical interference phenomena occurring in the nanoparticle layers that are embedded in its constituent 1DPCs. Thus, noteworthy, this film protects cells without the need of photodegradable dyes or absorbing inorganic particles, required in more traditional filters. This is advantageous because those components produce free radicals when exposed to UV radiation, which ultimately compromises the integrity, functionality, and biocompatibility of the latter filters. Thus, our results pave the way to new approaches of skin shielding against UV radiation, based on physical mechanisms that had never been used before for that purpose.

## Experimental Section

**Preparation of Particle Suspensions:** ZrO<sub>2</sub> nanoparticle sols were produced using a procedure based on the hydrolysis of zirconium *n*-propoxide, as reported in a previous study.<sup>[14]</sup> Briefly, zirconium *n*-propoxide (70%, Alfa Aesar) was added to Milli-Q water acidified with HNO<sub>3</sub> under strong stirring. Complete peptization of the precipitate was achieved in the same vessel, maintaining stirring at room temperature for approximately 72 h. The resulting colloidal suspension was dialyzed against pure Milli-Q water, using a 10 kDa molecular weight cut off dialysis membrane (Spectra/Por), until pH equaled 3.5. Finally, distillation at reduced pressure was employed to eliminate H<sub>2</sub>O. A suspension of ZrO<sub>2</sub> nanoparticles in methanol was then prepared, while commercial SiO<sub>2</sub> spherical nanobeads were obtained from Dupont (LUDOX TMA, Aldrich). TiO<sub>2</sub> particles were synthesized following a procedure described in the literature.<sup>[15]</sup> Briefly titanium tetraisopropoxide was added to water under stirring. Next, the resulting precipitate was placed in a tetramethylammonium hydroxide solution and incubated at 120 °C for 3 h. All nanoparticles were suspended in methanol and stored, with concentrations ranging from 1 to 4 wt%.

**Fabrication of 1D Photonic Crystals:** Photonic crystals were built by sequential and alternate deposition of ZrO<sub>2</sub> or TiO<sub>2</sub> particles and SiO<sub>2</sub> colloidal suspensions, following a procedure reported previously.<sup>[8]</sup> Suspensions were deposited over glass slides by means of a Laurell WS-400E-6NPP spin coater. For this, they were spun during 60 s, using final speeds between 4500 and 6000 rpm and an acceleration ramp of 11 340 rpm s<sup>-1</sup>. This procedure was followed repeatedly until the desired number of layers for each photonic crystal was casted.

**Polymer Infiltration Within the Multilayer Interstices and Lifting-Off:** A mixture of the elastomeric precursor of PDMS (0.5 g) and a curing agent (Sylgard 184, Dow Corning) was deposited and spin coated (40 s at 700 rpm) on top of the multilayered films above. Samples were then kept at room temperature for 24 h, to facilitate diffusion of the mixture throughout the pore network. After this, polymerization of PDMS was induced placing samples in a stove at 110 °C for 30 min. In order to lift them off the substrate, the resulting flexible photonic structures were first immersed in liquid nitrogen and then allowed to warm up to room temperature before separating them from the supporting slide.

**Optical and Structural Characterization of Films:** Total optical reflectance (RT) and transmittance (TT) spectra were measured using a spectrophotometer (SHIMADZU UV-2101PC) attached to an integrating sphere operating in the UV and visible range. Spectrophotometer slits were adjusted to collect the spectra from the same spot size in both modes. Absorbance (*A*) was estimated from these measurements using the expression  $A = 1 - (RT + TT)$ . Film pictures herein reported were taken using a digital camera (Pentax Kx). The microstructure of the

self-standing multilayered films was analyzed by using a microscope FESEM Hitachi 5200 operating at 5 kV. A very thin layer of gold (8 nm) was deposited on both faces of the self-standing film to avoid charge effects on the sample.

**Cell Culture:** The human SB2 cell line, isolated from a human primary cutaneous lesion, was kindly provided by Dr. Bar-Eli (M.D. Anderson Cancer Center, Houston, TX, USA).<sup>[16,17]</sup> Cells were grown in Dulbecco's modified Eagle's medium supplemented with 10% fetal bovine serum and 1% (v/v) penicillin–streptomycin–glutamine (10 000 units mL<sup>-1</sup> penicillin G sodium, 10 000 µg mL<sup>-1</sup> streptomycin sulfate and 200 × 10<sup>-3</sup> M L<sup>-1</sup> glutamine) (Gibco) at 37 °C and in a CO<sub>2</sub>-enriched (5%) atmosphere.

**UVB Irradiation:** UVB irradiation was carried out basically as described in previous studies.<sup>[18,19]</sup> Briefly, SB2 cells were seeded at 60% confluency in 96 multiwell plates 24 h before irradiation. Cells were then washed three times with phosphate-buffered saline (PBS) and kept in the same buffer during UV exposure to avoid the photosensitizing effect of the culture medium. UVB was irradiated using a 450 W ozone free Xenon Lamp and dichroic mirrors (Newport, Oriel Instruments), and neutral filters were used to adjust radiation to 2 J m<sup>-2</sup> s<sup>-1</sup> at a lamp-to-target distance of 23 cm, with the aid of a UVB detector attached to a photometer (Solar Light company Inc. USA). Using this experimental setup, samples were placed 23 cm away from the lamp, with the plate lids off but covered by films if appropriate, and irradiated for either 100 s or 500 s, to expose them to 200 or to 1000 J m<sup>-2</sup>, respectively. After irradiation, PBS was substituted by complete medium and cells were allowed to recover for 15 h in the incubator before analysis. Non-irradiated control cells were processed in the same way, except that they were not exposed to UVB light.

**Detection of CPDs:** CPDs were detected with the OxiSelect™ Cellular UV-Induced DNA Damage Staining Kit (Cell Biolabs Inc., USA), following manufacturer's instructions. Briefly, 15 h postirradiation, cells were fixed, and their DNA denatured, before incubating them with a primary anti-CPD antibody and, subsequently, with an appropriate secondary antibody conjugated to fluorescein isothiocyanate. Any unbound secondary antibody was removed by thorough washing. Samples lacking primary antibody or both primary and secondary antibodies were included as negative controls, to set up background fluorescence levels. Next, Hoechst 33342 (Invitrogen) (0.5 µg µL<sup>-1</sup>) were added to each well for 20 min, to stain nuclear DNA, and samples were examined using an automated, microscope-based, Operetta high content screening (HCS) system. Data were analyzed using the Harmony High Content Imaging and Analysis Software, from the same manufacturer as the Operetta System (Perkin-Elmer Inc.).

**Detection of Apoptosis:** The characteristic irreversible condensation of chromatin (pycnosis) that occurs during programmed cell death was used as a surrogate marker to identify apoptotic cells in our samples.<sup>[20]</sup> To do this, 15 h after UVB irradiation, cells nuclei were stained adding of Hoechst 33342 (Invitrogen) (0.5 µg µL<sup>-1</sup>) to our cultures for 20 min, and their morphology was analyzed using the automated Operetta HCS system (Perkin-Elmer). Nuclear fluorescence was quantified using the Harmony High Content Imaging and Analysis Software (Perkin-Elmer Inc.) and picnotic and nonpicnotic morphologies were identified and grouped accordingly using the Phenologic-Harmony software (Perkin-Elmer Inc.). Each experiment was performed three times and, for each one of them, samples were processed in quadruplicates. The Shapiro–Wilk test revealed a nonparametric distribution of our data, and therefore, we applied the Mann–Whitney test to determine the statistical significance of our results. Both tests were carried out using the R Software 3.0. Results were represented as box-and-whisker plots, with outlier values displayed as numbered white circles.

## Acknowledgements

R.N.-L. and B.P. contributed equally to this work. The authors thank Prof. Bar-Eli (MD Anderson Cancer Centre, Houston TX, USA) for kindly providing the human SB2 cell line. Research in the Dr. Guillermo de la

Cueva Méndez laboratory is supported by the Consejería de Igualdad, Salud y Políticas Sociales and the Consejería de Economía, Innovación, Ciencia y Empleo (BIO 3120), from the Junta de Andalucía, and by the Instituto de Salud Carlos III (FIS-2013, PI13/02753, cofinanced with European Regional Development Funds). Research in the Professor Míguez's laboratory leading to these results has received funding from the European Research Council under the European Union's Seventh Framework Programme (FP7/2007-2013)/ERC Grant Agreement No. 307081 (POLIGHT) and the Spanish Ministry of Economy and Competitiveness under grant MAT2011-23593.

Received: March 30, 2015

Revised: May 27, 2015

Published online:

- 
- [1] C. A. Cole, J. Vollhardt, C. Mendrok, *Clinical Guide to Sunscreens and Photoprotection* (Eds: H. W. Lim, Z. D. Draelos), Informa-Healthcare USA Inc., New York, NY **2009**, pp 39–51.
- [2] N. Serpone, D. Dondi, A. Albini, *Inorg. Chim. Acta* **2007**, *360*, 794.
- [3] J. Xiao, W. Chen, F. Wang, J. Du, *Macromolecule* **2013**, *46*, 375.
- [4] M. Zayat, P. Garcia-Parejo, D. Levy, *Chem. Soc. Rev.* **2007**, *36*, 1270.
- [5] K. Bolton, B. S. Martincigh, L. F. Salter, *J. Photochem. Photobiol.* **1992**, *63*, 241.
- [6] M. Nowick, A. Richter, B. Wolf, H. Kaczmarek, *Polymer* **2003**, *44*, 6599.
- [7] P. A. R. Yang, T. A. Christensen, J. R. Egerton, E. White, *Polym. Degrad. Stab.* **2010**, *95*, 1533.
- [8] J. R. Castro-Smirnov, M. E. Calvo, H. Miguez, *Adv. Funct. Mater.* **2013**, *23*, 2805.
- [9] M. E. Calvo, S. Colodrero, N. Hidalgo, G. Lozano, C. López, O. Sánchez-Sobrado, H. Míguez, *Energy Environ. Sci.* **2011**, *4*, 4800.
- [10] H. Ikehata, S. Higashi, S. Nakamura, Y. Daigaku, Y. Furusawa, Y. Kamei, M. Watanabe, K. Yamamoto, K. Hieda, N. Munakata, T. Ono, *J. Invest. Dermatol.* **2013**, *133*, 1850.
- [11] S. Mouret, C. Baudouin, M. Charveron, A. Favier, J. Cadet, T. Douki, *Proc. Natl. Acad. Sci. U.S.A.* **2006**, *103*, 13765.
- [12] S. Mouret, C. Philippe, J. Gracia-Chantegrel, A. Banyasz, S. Karpati, D. Markovitsi, T. Douki, *Org. Biomol. Chem.* **2010**, *8*, 1706.
- [13] J. F. Kerr, A. H. Wyllie, A. R. Currie, *Br. J. Cancer* **1972**, *26*, 239.
- [14] Q. Xu, M. A. Anderson, *J. Mater. Res.* **1991**, *6*, 1073.
- [15] S. D. Burnside, V. Shklover, C. Barbé, P. Comte, F. Arendse, K. Brooks, M. Grätzel, *Chem. Mater.* **1998**, *10*, 2419.
- [16] C. E. Verschraegen, B. C. Giovannella, J. T. Mendoza, A. I. Kozielsky, J. S. Stehlin, *Anticancer Res.* **1991**, *11*, 529.
- [17] R. K. Singh, M. Gutman, R. Reich, M. Bar-Eli, *Cancer Res.* **1995**, *55*, 3669.
- [18] T. A. Schwarz, V. F. Gschnait, T. A. Lugar, *J. Invest. Dermatol.* **1986**, *87*, 289.
- [19] T. T. Huynh, K. S. Chan, T. J. Piva, *Photodermatol. Photoimmunol. Photomed.* **2009**, *25*, 20.
- [20] V. Kumar, A. Abbas, F. Nelson, R. Mitchell, *Robbins Basic Pathology*, 8th ed., Vol. 6, Elsevier, **2007**, p 9, Table 1–1.
-